Developing and Validating Heat Exposure Products Using the U.S. Climate Reference Network

J. JARED RENNIE,[a] MICHAEL A. PALECKI,[b] SEAN P. HEUSER,[c] AND HOWARD J. DIAMOND[d]

[a] *North Carolina Institute for Climate Studies, North Carolina State University, Asheville, North Carolina*
[b] *NOAA/National Centers for Environmental Information, Asheville, North Carolina*
[c] *North Carolina State Climate Office, Raleigh, North Carolina*
[d] *NOAA/Air Resources Laboratory, College Park, Maryland*

(Manuscript received 15 December 2020, in final form 5 March 2021)

ABSTRACT: Extreme heat is one of the most pressing climate risks in the United States and is exacerbated by a warming climate and aging population. Much work in heat health has focused only on temperature-based metrics, which do not fully measure the physiological impact of heat stress on the human body. The U.S. Climate Reference Network (USCRN) consists of 139 sites across the United States and includes meteorological parameters that fully encompass human tolerance to heat, including relative humidity, wind, and solar radiation. Hourly and 5-min observations from USCRN are used to develop heat exposure products, including heat index (HI), apparent temperature (AT), and wet-bulb globe temperature (WBGT). Validation of this product is conducted with nearby airport and mesonet stations, with reanalysis data used to fill in data gaps. Using these derived heat products, two separate analyses are conducted. The first is based on standardized anomalies, which place current heat state in the context of a long-term climate record. In the second study, heat events are classified by time spent at various levels of severity of conditions. There is no consensus as to what defines a heat event, so a comparison of absolute thresholds (i.e., ≥30.0°, 35.0°, and 40.0°C) and relative thresholds (≥90th, 95th, and 98th percentile) will be examined. The efficacy of the product set will be studied using an extreme heat case study in the southeastern United States. While no heat exposure metric is deemed superior, each has their own advantages and caveats, especially in the context of public communication.

KEYWORDS: Climatology; Humidity; Temperature; Surface observations

1. Introduction

Heat is the deadliest annual weather-related hazard, causing an estimated average of 140 deaths per year (NWS 2020a), with some studies attributing approximately 5000 annual deaths to heat (Weinberger et al. 2020). Studies have shown heat-wave count, duration, and intensity increasing since the mid-twentieth century (Meehl and Tebaldi 2004; Perkins and Alexander 2013; Mora et al. 2017; Rennie et al. 2019; Keellings and Moradkhani 2020). According to Mora et al. (2017), 30% of the global human population is currently at risk of exposure to heat conditions exceeding a lethal threshold, and this percentage will increase to 48% and 74% by 2100 respectively under the low (RCP2.6) and high (RCP8.5) greenhouse gas emissions scenarios. While heat waves are often characterized by only using daily maximum temperature, it is well known daily minimum temperatures overnight can contribute to the dangerous health impacts of heat events (Nicholls et al. 2008; Habeeb et al. 2015; Nissan et al. 2017; Rennie et al. 2019). The persistence of heat exposure throughout the night has been shown to strongly impact people susceptible to extreme heat; for example, during the European heat wave of 2003 (Habeeb et al. 2015). Nissan et al. (2017) showed anomalously warm minimum temperatures caused increased mortality rates, as they inhibited people from getting enough sleep.

Studies have also shown heat and its effects on the human body are intensified by high levels of humidity, resulting in larger heat-related mortality and morbidity (Kalkstein and Davis 1989; Curriero et al. 2002; Willett and Sherwood 2012; Raymond et al. 2017; Limaye et al. 2018). When atmospheric moisture content is high, human sweat cannot evaporate efficiently, limiting the removal of latent heat from the body. This lack of evaporative cooling allows overall body temperature to reach higher levels when exposed to heat and/or physical activity (Sherwood 2018). Raymond et al. (2020) found some locales have already exceeded the upper physiological limit of humidity for human tolerance, with values of wet-bulb temperature T_w exceeding 35.0°C, although not for long durations. With an increase in both lower tropospheric temperature and humidity, it is expected the number of heat-wave events will increase by the end of the twenty-first century (Pachauri et al. 2014; Wuebbles et al. 2017; National Academies of Sciences Engineering and Medicine 2017). Limaye et al. (2018) estimate these increases could cause 12 000 excess deaths in the eastern United States by 2050.

a. Heat exposure measurement overview

Substantial work has been performed to better characterize heat impacts on humans. To account for heat and humidity, Steadman (1979, 1984) developed linear regression models to estimate the overall atmospheric heating impact called apparent temperature (AT). The equations are representative of several conditions (i.e., indoors, outdoor shade, and outdoor

Supplemental information related to this paper is available at the Journals Online website: https://doi.org/10.1175/JAMC-D-20-0282.s1.

Corresponding author: J. Jared Rennie, jared@ncics.org

DOI: 10.1175/JAMC-D-20-0282.1

sun) and are based on temperature, vapor pressure, and wind. It was initially developed for indoor conditions (Steadman 1979) but was modified to include outdoor conditions (Steadman 1984). The definition of outdoor AT is based on a mathematical model of an adult walking outdoors in the shade and includes factors such as heat generation and loss, fabric resistance, vapor pressure, wind speed, solar radiation, and proportion of body clothed. Although they are not used universally, NOAA's National Centers for Environmental Information (NCEI) provide AT data for public consumption, and these data were used by Grundstein and Dowd (2011) to examine trends in the United States and by Maier et al. (2014) to define heat exposure to develop a vulnerability index for Georgia. Habeeb et al. (2015) used AT at 50 U.S. metropolitan sites from 1961 to 2010 and showed that the average U.S. city experienced 0.6 additional heat waves per decade, a one-fifth-of-a-day increase in duration per decade, intensity increases by 0.1°C per decade, and an increase in the heat-wave season by 6 days per decade.

From the work of Steadman (1984), NOAA's National Weather Service (NWS) developed its own equation, commonly referred to as the heat index (HI; Rothfusz 1990). The HI was developed as a simplified version of AT that is based on temperature and relative humidity (RH), two parameters that are easily observed and reported. Since its implementation, it has become a popular metric and is used to issue NWS heat-related outlooks (Hawkins et al. 2017). Products are issued if HI values exceed a fixed, or absolute, threshold, which can vary between 40.6°C (105.0°F) and 48.9°C (120.0°F). These values vary by NWS office, and, while they do take into account local factors (sunlight, elevation, and time of day), there is no seasonal variation in these thresholds. Currently, efforts are under way by NWS to evolve its approach to issuing heat outlooks, starting in the western region of the United States, using measures relative to local and seasonal climatology (NWS 2020b).

While metrics such as AT and HI combine heat and humidity, they struggle to comprehensively diagnose heat stress, especially outdoors. Wet-bulb globe temperature (WBGT), originally developed by the U.S. military, is widely considered the most accurate indicator of heat stress on human health short of heat balance modeling (Yaglou and Minard 1957; Budd 2008, Lemke and Kjellstrom 2012, Patel et al. 2013). WBGT is comprehensive because it incorporates radiant heating and wind along with air temperature and humidity. WBGT is used by the U.S. Department of Defense, the U.S. Occupational Safety and Health Administration (OSHA), and athletic organizations, including the American College of Sports Medicine (ACSM). Although not adopted nationwide, some NWS Weather Forecast Offices (WFO) including Raleigh, North Carolina, and Tulsa, Oklahoma, utilize WBGT.

WBGT requires three inputs: dry-bulb temperature T, wet-bulb temperature T_w, and black-globe temperature T_g. The first two components (T and T_w) are easily observed and calculated, using temperature and humidity. However, direct measurement of T_g is done with specialized instrumentation, known as a black-globe thermometer (Fig. 1), that is not typical in standard meteorological station equipment. If this instrument is not provided, T_g must be estimated using heat mass and transfer algorithms, such as those

FIG. 1. Black-globe thermometer installed at the North Carolina ECONet Site in Rocky Mount, North Carolina. The image was provided by the NCSCO.

provided by Liljegren et al. (2008) and Dimiceli et al. (2013). Studies by Lemke and Kjellstrom (2012) and Patel et al. (2013) examined numerous T_g estimations and determined the one provided by Liljegren et al. (2008) gave the most valid results under outdoor conditions. Although not required, additional adjustments that are based on activity and clothing can be applied to WBGT to fully capture human heat stress (OSHA 2021).

WBGT has been of interest in recent climatological studies (Willett and Sherwood 2012; Grundstein et al. 2015; Heo et al. 2019; Carter et al. 2020). Grundstein et al. (2015) updated a categorical system of WBGT for use originally proposed by the ACSM and Georgia High School Association (GHSA). In a 4-yr study of heat stress in South Korea, Heo et al. (2019) found WBGT more accurately diagnosed extreme heat intensity and duration than air temperature did.

b. Goals of this paper

The U.S. Climate Reference Network (USCRN) is a systematic network of climate monitoring stations across the conterminous United States, Alaska, and Hawaii (Diamond et al. 2013). Stations are sited and installed in open areas expected to have stable land cover and use conditions for several decades to come. At each site, a suite of meteorological parameters is monitored, including triple redundancy for air temperature. Other variables recorded at USCRN sites include solar radiation, RH, and 1.5-m wind speed. Because these variables fully characterize outdoor heat exposure, the hourly and 5-min USCRN observations are valuable for testing heat-related indices at high temporal resolution, and for understanding the rural picture of heat exposure changes over time. This paper describes in detail the methods used to take hourly and 5-min USCRN data and derive AT, HI, and WBGT products. These heat exposure derivations, along with directly observed input variables, are tested and validated against values from nearby meteorological sites reporting similar variables.

Using the validated USCRN heat indices product, climatologies can be generated with methods developed to calculate hourly normals (Applequist et al. 2012). A method will be described that generates robust climatologies from shorter time series such as those of the USCRN (Leeper et al. 2019). From these climatologies, two separate analyses of heat exposure are conducted. First, standardized anomalies are used to place current heat state in the context of the climate record. Second, relative thresholds based on temperature distributions will be generated to examine cases of extreme heat. A case study of extreme heat is evaluated from an unseasonably warm event from a humid location in the southeastern United States.

The remainder of the paper is structured as follows. Section 2 describes the datasets used in the study, and section 3 describes the study method. The derived product, standardized anomalies, and case study are shown in section 4. Section 5 discusses caveats and limitations to heat indices, while section 6 summarizes the results and provides areas of future work.

2. Data

a. USCRN

USCRN is a network of 139 climate monitoring stations in the conterminous United States, Alaska, and Hawaii that collects high quality observations of meteorological variables relevant to heat-health studies such as air temperature, RH, solar radiation, and 1.5-m wind speed (Diamond et al. 2013). The sensors were deployed in 2001, with full CONUS coverage of 114 stations achieved in 2008; 23 stations have been installed across Alaska with an additional 2 stations in Hawaii. Temperature observations are recorded with triple redundancy by three independent platinum resistance thermometers of high accuracy that are housed in fan-aspirated triple-walled radiation shields. These configurations result in enhanced continuity and long-term accuracy of temperature observations, as the failure of one instrument leaves two more to continue observations. Other sensors include a capacitive thin-film polymer humidity sensor, a three-cup anemometer for wind speed at 1.5-m height above ground, and a silicon dome pyranometer to record solar radiation. Data are reported every hour, with 5-min observations beginning in 2009. Both hourly and 5-min data are used in this analysis.

b. Airport weather stations

For each USCRN station, the nearest airport weather station with similar data coverage was retrieved from the Integrated Surface Database (ISD; Smith et al. 2011). These data are from Automated Surface Observing System (ASOS) and Automated Weather Observing System (AWOS) stations owned by both the NWS and Federal Aviation Administration (FAA). Stations are maintained semiannually, and instruments include a hygrothermometer for temperature and dewpoint, a rotating cup anemometer for wind speed at 10-m height above ground, and a barometric pressure sensor. Data just before the top of the hour are retrieved for this study.

c. North Carolina ECONet

In addition to comparing with ASOS stations, a local-scale study is conducted at two sites in North Carolina, using observations from the Environment and Climate Observing Network (ECONet). The North Carolina ECONet, operated by the North Carolina State Climate Office (NCSCO), consists of 43 weather stations across the state, reporting information every minute. These stations are generally located at agricultural research stations, and the stations residing in Mills River and Durham, North Carolina, are within a few kilometers of a USCRN station (2.1 and 4.7 km, respectively). These stations report typical weather conditions such as temperature, humidity, and wind. Holder et al. (2006) made comparisons with ECONet stations and stations operated by the NWS Cooperative Observer Program (COOP) and showed that daily maximum and minimum temperature agreed well, with Pearson correlations of 0.96 and 0.89, respectively. In 2018, these sites were augmented with a black-globe thermometer (Fig. 1) to aid in making direct observations of WBGT.

d. Reanalysis data

To fill in data gaps, 0.25° hourly reanalysis data from the European Centre for Medium-Range Weather Forecasts (ECMWF), known as ERA5 (Copernicus Climate Change Service 2017) is used. To estimate WBGT, surface pressure is required. Since USCRN does not record pressure, it was extracted from the grid point in ERA5 closest to each station. In a similar fashion, surface solar radiation was extracted to accommodate ASOS stations, which do not have a pyranometer installed.

3. Method

a. Calculating heat exposure

For the USCRN and ASOS stations used in this study, heat exposure is calculated as follows. The HI is calculated based on the Rothfusz (1990) method used by the NWS. The equation is a polynomial fit to the apparent temperature using only air temperature and RH inputs:

$$\mathrm{HI} = -42.379 + 2.049\,015\,23 \times T + 10.143\,331\,27 \times \mathrm{RH} - 0.224\,755\,41 \times T \times \mathrm{RH} - 0.006\,837\,83 \times T^2 - 0.054\,817\,17 \times (\mathrm{RH})^2 + 0.001\,228\,74 \times T^2 \times \mathrm{RH} + 0.000\,852\,82 \times T \times (\mathrm{RH})^2 - 0.000\,001\,99 \times T^2 \times (\mathrm{RH})^2,$$

where RH is the relative humidity (%), and T is the dry-bulb temperature (°F). There are two adjustment factors applied to the HI under certain conditions in which the basic formula fit is less accurate. The first is if RH is less than 13% and the dry-bulb temperature is between 26.7° and 44.4°C. The second adjustment occurs if the RH is greater than 85% and the dry-bulb temperature is between 26.7° and 30.6°C. For cases in which the heat index is below 26.7°C (80°F), the equation is simplified as

$$\mathrm{HI} = 0.5\{T + 61.0 + [1.2(T - 68.0)] + (\mathrm{RH} \times 0.094)\}.$$

There are several varieties of AT. The outdoors in shade equation of AT from Steadman (1984) is used in this study:

$$\mathrm{AT} = -2.7 + 1.04T + 2e - 0.65v_{10},$$

where T is the dry-bulb temperature (°C), e is the vapor pressure (hPa), and v_{10} is the wind speed at 10 m (m s^{-1}). Because USCRN records wind speed at 1.5 m, an exponential adjustment factor is applied to match winds at 10 m, where surface roughness and stability is not a factor. The shade version of AT is used by necessity, as the version for heat exposure in direct sunlight requires information not provided as standard meteorological variables.

The component equation used to calculate WBGT is as follows from Yaglou and Minard (1957):

$$\mathrm{WBGT} = 0.7T_w + 0.2T_g + 0.1T,$$

where T_w is the natural wet-bulb temperature, T_g is the globe temperature, and T is the dry-bulb temperature, all in degrees Celsius. The biggest limitation to using WBGT for climatological studies is that it incorporates T_g, whose measurement requires a black-globe thermometer that is not standard (Fig. 1).

Over the years, various T_g estimation formulas have been developed and compared with direct black-globe thermometer measurements. These efforts include work with the Argonne National Laboratory by Liljegren et al. (2008), and the NWS by Dimiceli et al. (2013). Both of these estimations primarily used standard surface variables as input data and use heat and mass transfer algorithms to calculate T_g. Both methods were found to be reasonably accurate over small regions and short time periods. As examples, the Liljegren method exhibited an accuracy of 1.0°C or better at military depots in seven states, and the Dimiceli method has been tested within an accuracy of 0.6°C in the Tulsa, Oklahoma, area, during September 2010 and July 2011. These independent methods are applied and tested at USCRN sites. The Liljegren method uses air temperature, RH, wind speed, solar radiation, and surface pressure as inputs, and both T_g and T_w are modeled using fundamental principles of heat and mass transfer. This, combined with air temperature, is used to calculate WBGT. Inputs for the Dimiceli method are similar, with the exception of dewpoint temperature instead of RH. This method only calculates T_g, and to calculate T_w the equation from Stull (2011) was used, using T and RH as inputs:

$$T_w = T\,\mathrm{atan}[0.151\,977(\mathrm{RH} + 8.313\,659)^{1/2}] + \mathrm{atan}(T + \mathrm{RH}) - \mathrm{atan}(\mathrm{RH} - 1.676\,331) + 0.003\,918\,38(\mathrm{RH})^{3/2}\,\mathrm{atan}(0.023\,101 \times \mathrm{RH}) - 4.686\,035.$$

Directly observed T, modeled T_g from Dimiceli et al. (2013), and estimated T_w from Stull (2011) are combined to make a secondary version of WBGT, hereby referred to as the effective Dimiceli method.

b. *Validation using nearby networks*

Hourly USCRN heat exposure values are compared with nearby stations in the ASOS network. Distances between neighboring stations varied from 0.6 to 142 km. The six stations with the furthest distances (over 80 km) were in remote areas of Alaska. Estimated values of HI, AT, and WBGT are compared, as well as the input measurements of temperature, humidity, and wind at or adjusted to the standard 10-m height above ground level. Since ASOS stations do not report solar radiation, these data were taken from the nearest grid in ERA5. Pearson's correlation is calculated between the two networks for validation. Root-mean-square error (RMSE) and bias are also calculated and are provided as online supplemental material. Results are stratified by all cases, daytime, nighttime, and heat event cases. A heat event here follows the work of Meehl and Tebaldi (2004); it must exceed the 98th percentile for five consecutive hours, and it must occur for at least three consecutive days. While HI, AT, and WBGT are estimated at both networks, understanding local and climatological variations in these estimates (and directly observed inputs) are important to note, and can be used to aid in calibration of future WBGT estimation algorithms.

In addition to the national validation analysis, a local analysis is included for two USCRN stations in North Carolina (Asheville and Durham) within 2.1 and 4.7 km of stations (Fletcher and Chapel Hill) in the ECONet, respectively. These stations not only have all the required variables to estimate WBGT, but also have black-globe thermometers and pyranometers installed, so direct measurements of WBGT and solar radiation can be compared with USCRN estimated WBGT and measured solar radiation.

c. *Quantifying heat severity*

Regardless of metric used, it may prove valuable to quantify heat exposure indices in the context of station histories. The heat vulnerability of a population may vary with respect to the conditions to which it is normally exposed. Standardizing absolute observations can provide a relative measure of conditions that account for locational and seasonal variations. The most common approach is based on a climatology derived

TABLE 1. Pearson's correlation of HI and AT between USCRN and neighboring stations, stratified by geography, time of day, and whether heat conditions are extreme. All rows examine correlations between USCRN and ASOS, with the exception of the North Carolina row, which examines USCRN and nearby ECONet sites.

	All data	Daytime	Nighttime	Extreme (daytime)	Extreme (nighttime)
All (HI)	0.93	0.93	0.91	0.90	0.84
Southeastern United States (HI)	0.96	0.97	0.96	0.95	0.92
Southwestern United States (HI)	0.80	0.78	0.76	0.64	0.65
North Carolina (HI)	0.98	0.98	0.97	0.98	0.93
All (AT)	0.91	0.91	0.91	0.86	0.84
Southeastern United States (AT)	0.96	0.96	0.96	0.93	0.92
Southwestern United States (AT)	0.78	0.75	0.73	0.62	0.65
North Carolina (AT)	0.97	0.96	0.95	0.96	0.92

from a reference period (Arguez et al. 2012). Temperatures from NCEI's Global Historical Climatology Network (GHCN; Menne et al. 2012) and nClimGrid (Vose et al. 2014) are often compared with their respective climatologies in climate monitoring reports. Traditionally, a climatology of 30 years is required; however, shorter periods of record have been used where a longer period record is not available. For example, the last set of official U.S. climate normals (1981–2010) also provided an hourly supplemental normal based on 10 years of information using data exclusively from the recently deployed U.S. ASOS (Applequist et al. 2012). This short-term climatology was generated using a sampling of hourly measurements over a 15-day window for each day-of-year hour over the period of record (Applequist et al. 2012). These hourly normals have been shown to provide adequate information, and the methodology has been used in standardizing other short-duration datasets, including soil moisture (Leeper et al. 2019).

Another method for quantifying heat severity is comparing the indices to thresholds. There is no single universal definition of extreme heat, but it can be generalized as a period where conditions exceed a critical threshold value (Robinson 2001; Perkins and Alexander 2013). These thresholds can be absolute in nature (i.e., ≥30.0°, 35.0°, and 40.0°C) or relative, the latter using standardized anomalies (i.e., ≥+1 standard deviation) or percentiles (≥90th, 95th, and 98th). While numerous absolute and relative based thresholds have been examined, there is not one unified method for determining health outcomes from heat events (Perkins and Alexander 2013; Vaidyanathan et al. 2016; Smith et al. 2013). A study by Grundstein et al. (2015) used relative WBGT thresholds to estimate heat stress severity across athletic organizations in the United States. NWS procedures (Hawkins et al. 2017) utilize absolute thresholds to issue heat-related outlooks for much of the United States.

Using hourly heat data from USCRN, normals are calculated in a similar manner to Applequist et al. (2012). Each hourly normal was computed on the basis of the number of possible values between 2009 and 2019, with a requirement to have three years of data available. Creating the climatology was done by aggregating over a particular date and time, ±7 days, over the station periods of record. If more than 20% of data were missing, the hourly normal was set to missing. The number of possible values depend on the station periods of record, ranging between 45 (3 years) and 165 (11 years). If there was enough data, the arithmetic mean was computed and considered the hourly climatology. Also, the 90th, 95th, and 98th percentiles were calculated from the available hourly data, using a normal Gaussian distribution. These percentiles are normally used when examining heat-intensity events (Meehl and Tebaldi 2004; Perkins and Alexander 2013; Rennie et al. 2019). Anomalies (observation–climatology) and standardized anomalies (anomaly divided by standard deviation) are calculated for assessment.

d. *Case study*

The performance of this set of heat exposure indices was examined for an event located in the southeastern United States, which experiences higher humidity because of its proximity to the Gulf of Mexico and Atlantic Ocean and prevailing southerly winds. An early October 2019 event is evaluated in the piedmont areas of North Carolina, as air temperatures reached 37.8°C (100.0°F) on 3 October. For the case study, hourly and 5-min T, AT, HI, and WBGT values are shown and examined. In addition, standardized climatologies and percentiles are examined to quantify event severity. The application of absolute versus relative heat measures during this event is discussed.

4. Results

a. *Validation of USCRN heat exposure indices to nearby networks*

Table 1 list the correlations between USCRN HI and AT against nearby weather stations. Results are stratified geographically by all USCRN stations, as well as stations in the southeastern United States, southwestern United States, and North Carolina. These subregions are shown because of the dominant prevalence of humidity (Southeast) or lack thereof (Southwest). An additional analysis is provided for North Carolina, where two USCRN stations are analyzed against a pair of ECONet stations. The results are also stratified by daytime and nighttime hours on all days and during extreme events, defined as exceeding the 98th percentile for five consecutive hours, and it must occur for at least three consecutive days.

Overall, results for HI and AT are strongly positively correlated for all stations, as the diurnal cycle of all these indices typically generate strong relationships. The all-station category

TABLE 2. As in Table 1, but for WBGT (Liljegren 2008; Dimiceli 2013).

	All data	Daytime	Nighttime	Extreme (daytime)	Extreme (nighttime)
All (Liljegren)	0.89	0.84	0.93	0.68	0.88
All (Dimiceli)	0.93	0.94	0.92	0.91	0.88
Southeastern United States (Liljegren)	0.92	0.90	0.96	0.78	0.94
Southeastern United States (Dimiceli)	0.97	0.97	0.96	0.96	0.93
Southwestern United States (Liljegren)	0.80	0.67	0.78	0.49	0.65
Southwestern United States (Dimiceli)	0.81	0.78	0.77	0.63	0.66
North Carolina (Liljegren)	0.94	0.88	0.93	0.88	0.84
North Carolina (Dimiceli)	0.77	0.61	0.93	0.59	0.81

demonstrates this with a correlation coefficient of 0.93. Correlations are lower at nighttime, especially during extreme event cases. This is likely due to local variations in RH at night, which can be affected by surrounding land cover and topography. The southeastern United States performs very consistently, with correlation coefficients above 0.92 across the board. However, the southwestern United States does not perform as well, with correlations no higher than 0.80. This is possibly due to elevation and topographic differences between neighboring stations, as the western United States is generally more mountainous. Another factor is lower humidity in these areas, and the assumptions within the HI equation set for low humidity conditions. The equation used by Rothfusz (1990) has an adjustment factor when RH is lower than 13%, which frequently occurs in arid areas. In general terms, heat events in the southwestern United States are primarily dominated by air temperature, and incorporating the HI provides a lower value than temperature due to evaporative cooling accounted for by the model on which the HI is based. This can be counterintuitive from a communications perspective. Table S1 in the online supplemental material provides RMSE and bias values and are consistent with correlation results. HI biases range between −2.70 and 0.87 and RMSE between 0.70 and 8.37. The highest RMSE values correspond to the lowest correlations, in the western United States, AT results are generally similar in pattern but with lower correlation magnitudes (and higher RMSE values) than their HI counterparts. While HI and AT both incorporate temperature and humidity, AT also includes wind. Wind speed can vary substantially by location and can cause differences in the resulting AT value between USCRN and ASOS stations, especially at nighttime when wind speeds are low. AT calculations are very sensitive to low wind speeds. Nonetheless, correlations are still very strong for the southeastern United States, with values above 0.92.

Table 2 provides USCRN to ASOS/ECONet comparison results for the two estimation methods of WBGT. For all data, results are generally strong with correlation coefficients of 0.89 for the Liljegren method, and 0.93 for the Dimiceli method. Table S2 in the online supplemental material provides RMSE and bias values and are consistent with correlation results. These two WBGT methods appear to have similar correlation results to those of HI and AT. As expected, correlations in the southwestern United States are not as strong, due to lower humidity and differences in topography. Daytime extreme events have the lowest correlations when comparing USCRN with ASOS/AWOS stations using the Liljegren et al. (2008) method. Correlations of 0.68, 0.78, and 0.49 exist for all, southeastern and southwestern USCRN stations, respectively, with RMSE values of 7.08, 7.42, and 7.38, respectively. This is possibly due to the use of ERA5 for solar at ASOS stations. ERA5 is on a 0.25° grid and may not resolve mesoscale variations in cloud cover. The Dimiceli method yields a higher correlation than the Liljegren method in all cases, with the exception of North Carolina stations. Here, the Liljegren method performs well, with 0.94 (6.02 RMSE) in all cases, and 0.88 (7.15 RMSE) in extreme daytime cases comparing USCRN estimates to a pair of stations that directly measures all the components in the WBGT.

To contextualize the variation in results, variables used to calculate HI, AT, and WBGT, are shown in Table 3. As expected, temperature is the best performer in most cases, since it is a spatially continuous variable. The exception is the Southwest, as it has a correlation of 0.80, while surface pressure, another spatially continuous variable, is higher (0.88). The variable with the lowest correlation is wind, with coefficients ranging between 0.20 and 0.34, even after adjusting USCRN 1.5-m winds for elevation above ground to match ASOS 10 m winds. Wind is not spatially continuous at the surface due to friction and local terrain characteristics. When comparing USCRN sites with ASOS/AWOS stations, surface pressure and solar radiation are taken from the ERA5 reanalysis model dataset. Results are generally good for surface pressure, with correlations between 0.81 and 0.83. Results varied with solar radiation, with correlation correlations between 0.69 and 0.82. RMSE values (provided in Table S3 in the online supplemental material) were large, varying between 126 and 176 for ASOS comparisons, and 35–40 for ECONet. As stated previously, small variations in cloud cover may not be resolved on ERA5 grids, thus affecting solar radiation results. Nonetheless, while the use of direct observations is ideal, filling in gaps with reanalysis data can be an acceptable alternative.

Although only two station pairs are available in the North Carolina analysis, it appears all variables are better correlated between USCRN and ECONet stations than to ASOS/AWOS stations, as they were located within 5 km and at similar elevations. This is especially true with wind, as their correlation coefficients are much higher than ASOS/AWOS counterparts, ranging between 0.55 and 0.67 (and RMSE between 0.29 and 0.61). Solar radiation correlations were very high as direct observations were gathered at both locations and were not reliant on reanalysis data over a broader region. The closest

TABLE 3. As in Table 1, but for input variables for WBGT calculations. Asterisks indicate variables that were sourced from ERA5 output for either USCRN (air pressure) or ASOS (solar radiation).

		All data	Daytime	Nighttime	Extreme (daytime)	Extreme (nighttime)
All	*T*	0.92	0.92	0.89	0.88	0.82
	RH	0.82	0.84	0.74	0.81	0.74
	Pressure*	0.81	0.81	0.81	0.81	0.83
	Wind	0.34	0.34	0.28	0.21	0.20
	Solar*	0.82	0.69	—	0.69	—
Southeastern United States	*T*	0.96	0.97	0.96	0.94	0.92
	RH	0.74	0.76	0.48	0.77	0.53
	Pressure*	0.76	0.76	0.77	0.70	0.75
	Wind	0.40	0.36	0.38	0.10	0.11
	Solar*	0.79	0.66	—	0.68	—
Southwestern United States	*T*	0.80	0.78	0.74	0.65	0.66
	RH	0.76	0.75	0.73	0.59	0.67
	Pressure*	0.88	0.88	0.87	0.89	0.89
	Wind	0.17	0.21	0.12	0.09	0.06
	Solar*	0.86	0.72	—	0.74	—
North Carolina	*T*	0.98	0.98	0.96	0.98	0.93
	RH	0.94	0.96	0.93	0.97	0.95
	Pressure	0.87	0.87	0.88	0.89	0.90
	Wind	0.67	0.62	0.55	0.67	0.56
	Solar	0.97	0.95	—	0.95	—

ASOS stations varied between 1 and 80 km and may have differing elevations, especially in the western United States. For accurate comparisons, it is ideal for stations to be as close together as possible, with similar, direct observations. As a result, the Liljegren method to calculate WBGT outperforms the Dimiceli method at these two sites. Lemke and Kjellstrom (2012) and Patel et al. (2013) showed the Liljegren method was the best model to calculate WBGT, especially in outdoor conditions. For these reasons, the final production of USCRN WBGT uses the Liljegren et al. (2008) estimation method.

b. *Quantifying heat severity using standardized anomalies and heat thresholds*

Hourly climatologies and percentile thresholds of *T*, HI, AT, and WBGT are generated using methods described in Applequist et al. (2012). Table 4 displays the 98th-percentile thresholds, averaged by region, for the months of May–October. This calculation was done for afternoon hours, between 1200 and 1800 local time. The high percentile thresholds peak in July as expected, with a considerable fall off in October relative to the other warm-season months May–September. With a warming climate, it is expected late spring and early autumn months will have an increased probability of warm temperature extremes, which can have impacts on health and agriculture (Wuebbles et al. 2017). In looking at the southeastern and southwestern regional averages, note that the 98th-percentile values are generally in the low to mid-30°C. The NWS uses considerably higher absolute thresholds in most areas of the United States beginning with an HI of 40.6°C (105.0°F) to administer heat outlooks (Hawkins et al. 2017).

In general, HI and AT values are higher than their temperature counterparts, especially in the midsummer period. By adding the effects of humidity, a person's "feels like" temperature is increased. The exception to this is the southwestern United States, where temperature is dominant in the area, and lower RH values lead to a decrease in HI, a common issue in the area. While the units of WBGT (°C) are the same as the other exposure products, they are systematically lower in most cases. This property is a well-known result of the combinatorial weights in the WBGT equation; however, these lower values can be perceived differently by the public with regards to severity. This is explored in more detail in the discussion section.

Figure 2 depicts a geographic view of the July 98th percentiles for the heat indices. As expected, higher temperature thresholds exist in southern regions of the United States. The percentile value for temperature can vary between 19.6° and 49.3°C (67.3°–120.7°F). Values are similar for both HI and AT, ranging between 19.4° and 45.0°C (67.0°–113.0°F), and 19.7° and 47.6°C (67.5°–117.7°F), respectively. WBGT values tend to

TABLE 4. The 98th-percentile thresholds (°C) of afternoon (1200–1800 local time) *T*, HI, AT, and WBGT at USCRN sites, averaged by region, using a standardized climatology method, for the months between May and October.

		May	Jun	Jul	Aug	Sep	Oct
T	All	27.3	30.9	32.2	31.1	28.9	23.5
	Southeast	31.0	33.5	34.1	33.5	32.5	29.0
	Southwest	28.9	33.3	34.3	33.3	31.4	26.1
HI	All	26.8	31.1	33.0	31.8	28.9	23.0
	Southeast	32.3	36.8	38.5	38.0	35.0	30.7
	Southwest	26.8	30.8	32.1	31.3	29.5	24.5
AT	All	25.5	30.0	31.8	30.8	28.1	21.8
	Southeast	31.6	35.0	36.0	35.6	34.0	29.8
	Southwest	25.7	30.8	32.3	31.4	29.2	23.6
WBGT	All	24.4	27.6	29.0	28.1	25.8	20.7
	Southeast	29.6	32.0	32.8	32.5	30.5	27.2
	Southwest	23.3	26.1	27.6	27.1	25.3	21.0

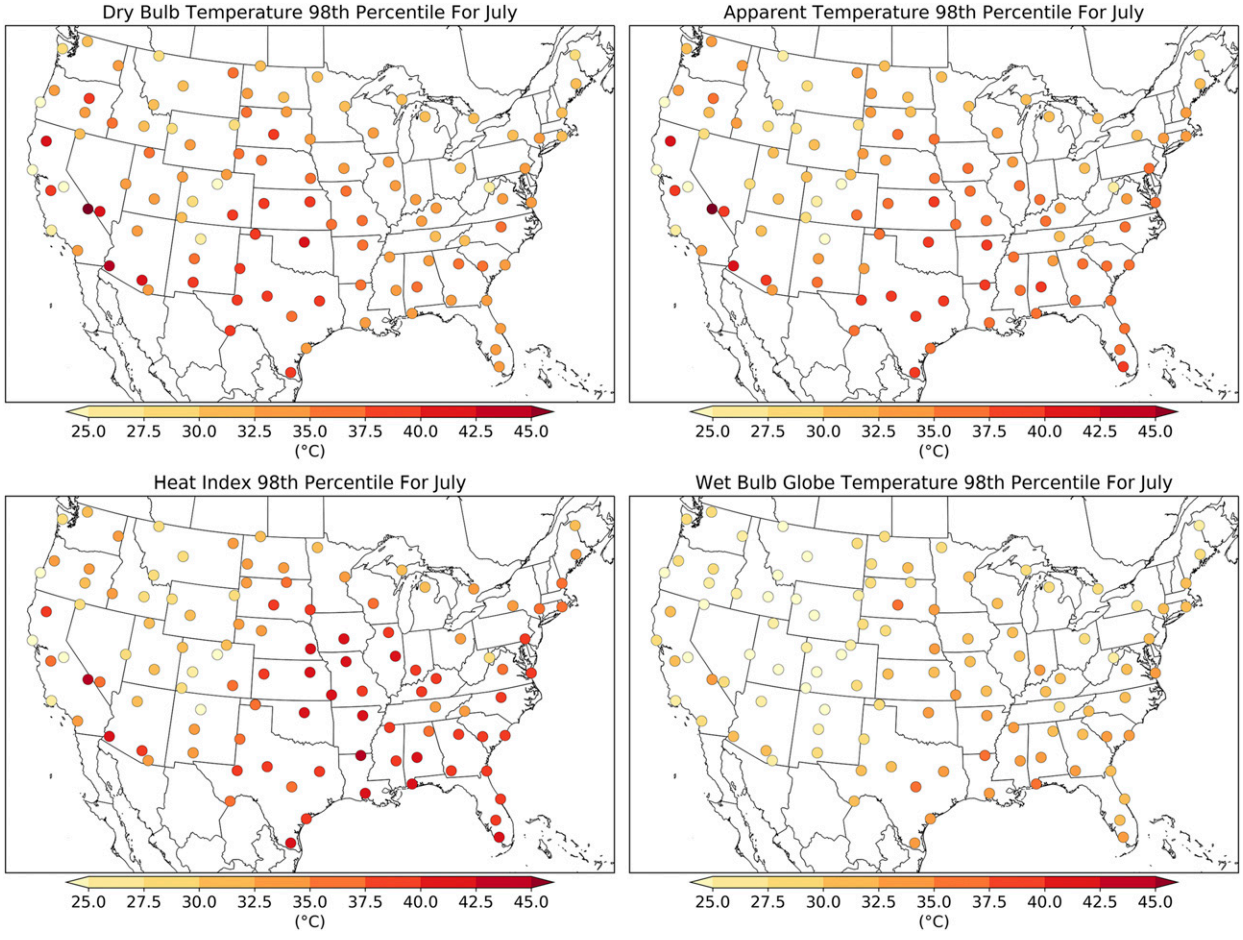

FIG. 2. Climatological 98th percentile (°C) of July afternoon (1200–1800 local time) *T*, AT, HI, and WBGT data at USCRN sites.

be lower than T, HI, and AT, with a range between 23.0° and 37.4°C (73.4°–99.3°F). This can have implications if WBGT is used for communicating heat information to the public, as it can be perceived that a dangerous value of WBGT (e.g., 32.2°C or 90.0°F) is not unusual or impactful enough to alter plans for outdoor activities.

As seen in Fig. 2, the 98th percentile can vary considerably in short distances, especially in areas with considerable elevation change. For example, in July the HI 98th percentile in Durham is 38.3°C (101.0°F). In North Carolina, an HI of 40.6°C (105.0°F) is needed to trigger an excessive heat warning (Hawkins et al. 2017). While 40.6°C is above the 98th percentile, it is well within the statistical range of possibilities. However, in Asheville, a city in the mountainous western portion of North Carolina, the July HI 98th percentile is only 32.7°C (90.8°F). Therefore, the 40.6°C criteria for a heat-related advisory to be issued by the NWS is rare. In fact, archives going back to 1986 show there have been little to no heat-related advisories issued in western North Carolina (Fig. 3; Iowa Environmental Mesonet 2020).

Another way to attribute the difference between absolute and relative thresholds, Figs. 4 and 5 are plotted examining the duration of time spent at levels of high heat in 2012 using absolute and relative thresholds, respectively. The year 2012 is the warmest on record nationally overall, and the second warmest for overnight temperatures. If using an absolute threshold of 32.5°C (90.5°F), virtually all hours exceeding this

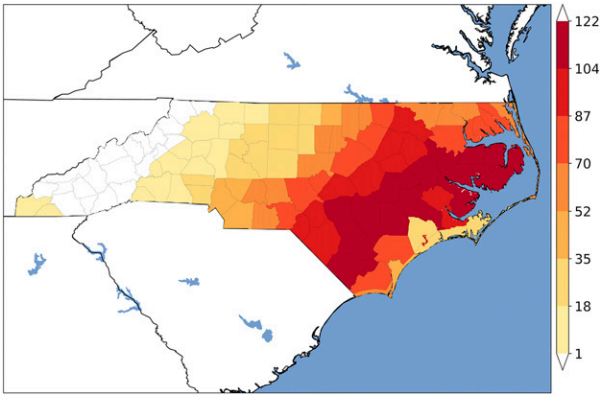

FIG. 3. Number of heat advisories issued by NWS offices for the state of North Carolina between 1986 and 2020. Data are from Iowa Environmental Mesonet (2020).

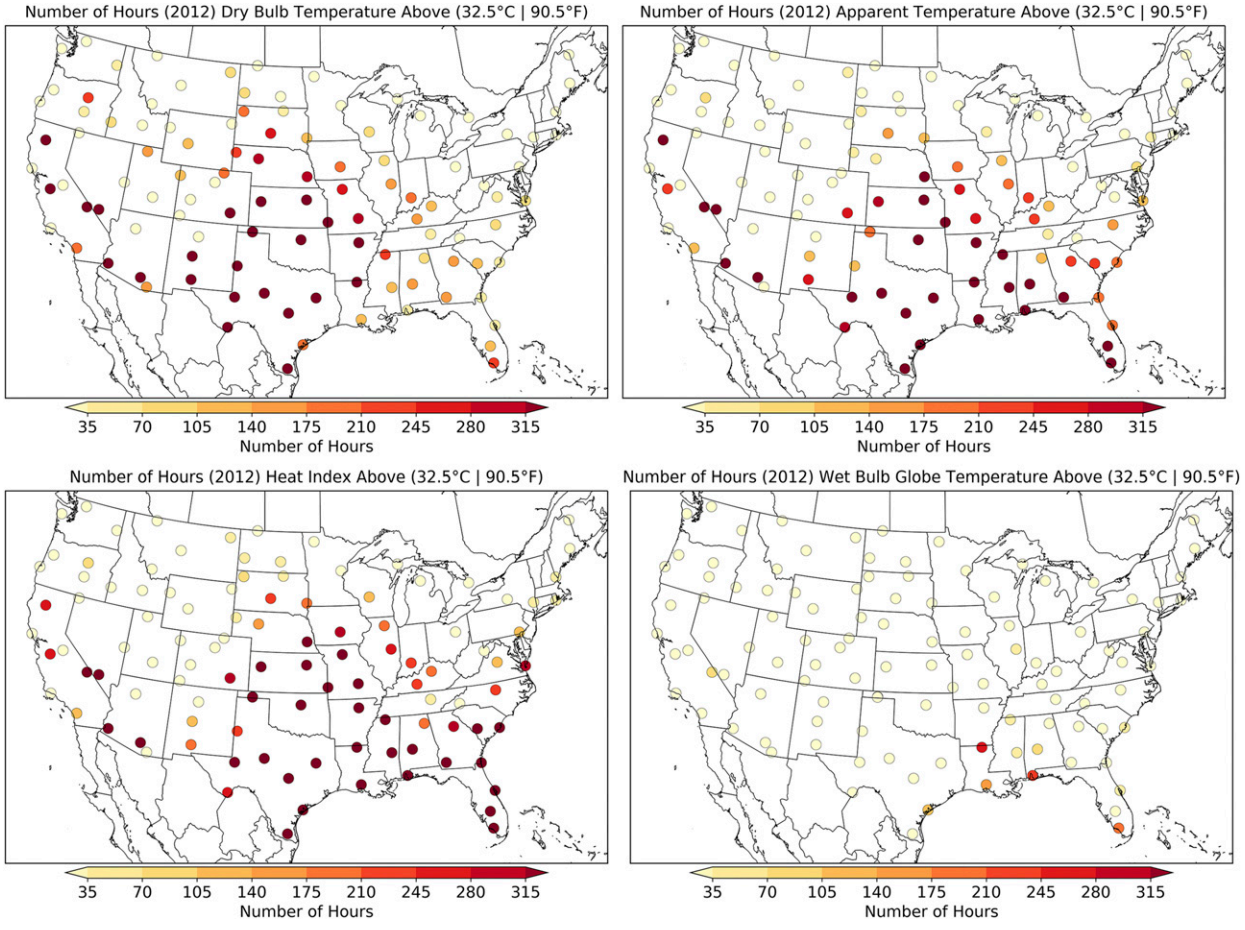

FIG. 4. Number of hours in 2012 that *T*, AT, HI, or WBGT was greater 32.5°C (90.5°F).

level exist in the southern parts of the United States, where temperatures are normally warmer. If, instead, a relative threshold is used (95th percentile, Fig. 5), it can be shown that high heat periods can happen at virtually every USCRN site. This is especially true for the upper Midwest regions of the United States, which were experiencing an exceptional drought in 2012. WBGT would also benefit from a relative threshold since its values are typically lower.

c. *Case study: Autumn 2019 heat in the southeastern United States*

On 3 October 2019, high pressure off the coast of North Carolina provided an unseasonably warm day for the southeastern United States. Raleigh–Durham airport reached a daily maximum temperature 37.7°C (100.0°F) in the afternoon, which not only became a record for that day but was also the highest temperature recorded in Raleigh for the 2019 year. Figure 6 displays the time series of temperature, HI, AT, and WBGT for the Durham, North Carolina, USCRN station (approximately 29 km from the Raleigh–Durham airport) for 3 October. According to the station's climatology, 3 October is expected to be in the low 20°s to mid-20°s in Celsius for all variables. On 3 October 2019, the temperature surpassed 32.2°C (90.0°F) for over 6 h, with a maximum of 36.3°C (97.3°F) at around 1500 local time. RH values were generally low for the day (between 27% and 35% for most of the day). As a result, HI and AT values never surpassed 36.7°C (98.0°F). The hourly values of AT and WBGT have more variation when compared with the *T* and HI counterparts because of the varying nature of wind and solar. This is especially seen in the 5-min data and appears to be removed when applying a 15-min smoothing function. WBGT experienced a sharp increase in the morning as the sun came out. The maximum WBGT value was 30.8°C (87.5°F), which according to athletic risk categories in Grundstein et al. (2015), athletes should "limit intense exercise and total daily exposure to heat and humidity."

Table 5 places the maximum heat exposure recordings and in context to its climatology. The standardized anomaly (anomaly divided by the standard deviation) is around two standardize units or higher for all variables, a considerably warm event for this time of year. The maximum recorded value also exceeded the station 98th percentile value for October daytimes. While heat was mentioned in the forecast products from the NWS such as hazardous weather outlooks and area forecast discussions for this day, no heat advisory or warning was issued, because the HI threshold of 40.6°C (105.0°F) was

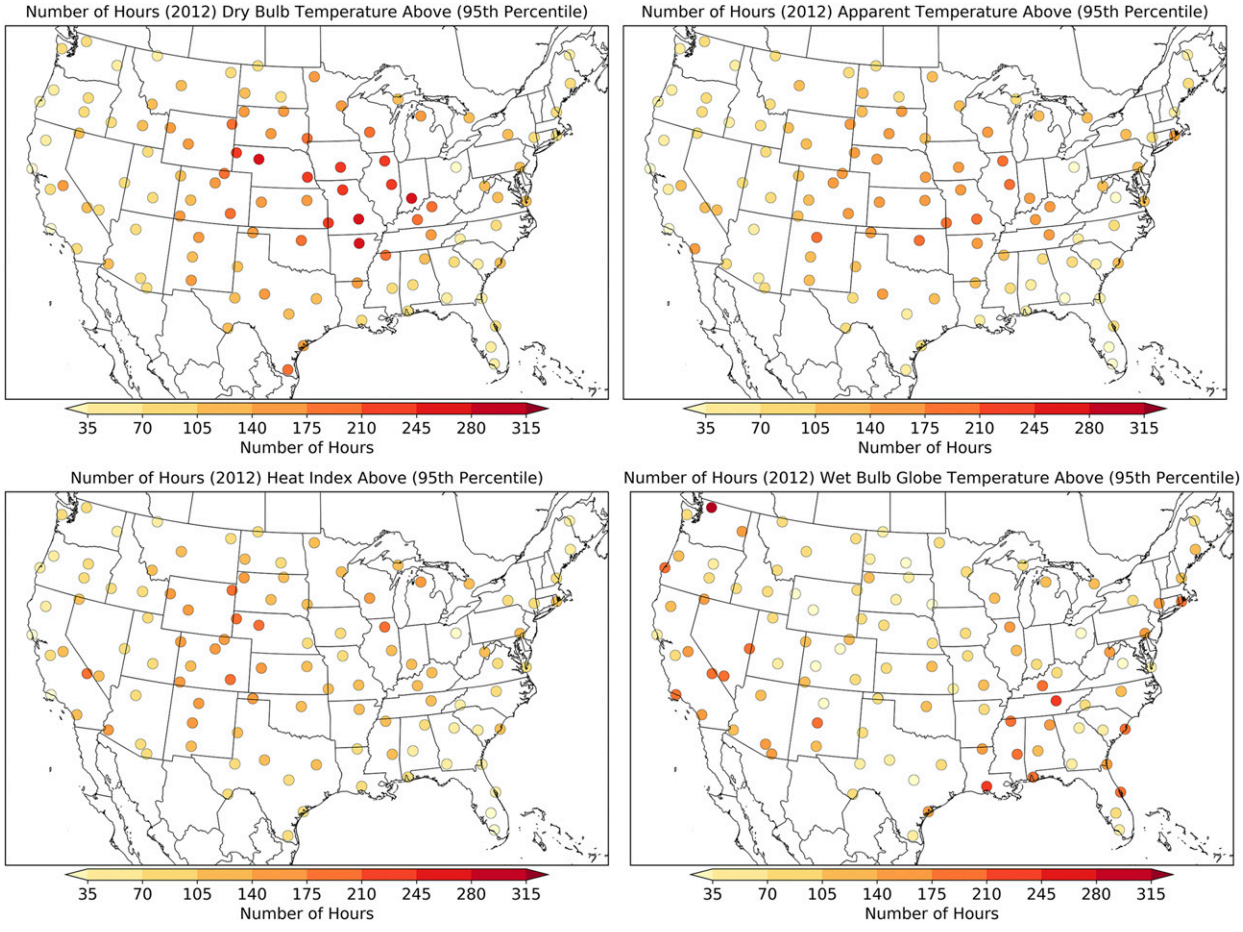

FIG. 5. Number of hours in 2012 that *T*, AT, HI, or WBGT was greater than the station's 95th percentile for that given hour.

not reached (Hawkins et al. 2017). However, HI was 5.0°–8.0°C above the 98th percentile, which is substantially hazardous for early October. If percentile metrics were used, it would have been clear that these conditions warranted notification for student athletics and other outdoor activities to be curtailed.

5. Discussion

a. Heat exposure measurement assumptions

The HI is a widely accessible, easy-to-develop heat product. It is also the best metric when validating USCRN data to nearby ASOS/AWOS sites. However, the equation used (Rothfusz 1990) assumes a person is in the shade and experiencing light winds. In the presence of direct sunlight, the human feels-like temperature can be higher because of the body absorbing incoming solar radiation. As a result, HI may not be the best metric for outdoor conditions, especially when there is no shade available. Additionally, numerous assumptions are made when calculating the HI value, including special conditions not met well by the original regression equation, such as low humidity. As a result, the HI value is inadequate for some conditions in the western areas of the United States, where RH values can typically be less than 10% during summer. For example, on 16 August 2020 the Cooperative Observer (COOP) weather station at the Death Valley National Park Service Visitors Center in Furnace Creek, California, recorded a high air temperature of 54.4°C (130°F) at 1541 local time. At the same time, a nearby USCRN site in Stovepipe Wells, California, recorded a maximum temperature of 51.5°C (124.7°F). The RH values were less than 10% during the day, and as a result the highest HI recorded at each site was only 44.4°C (112.0°F). NWS offices in the western United States rarely use HI, and their new product, known as NWS Heat Risk, only incorporates temperature (NWS 2020b).

The AT version most typically used assumes shaded conditions outdoors, and also would underestimate heat exposure in direct sunlight. Steadman (1984) did produce alternative version of AT that included sunlight effects, but these do not utilize standard values that are currently observed or easily estimated. While wind is represented in the form of the equation used here, it is highly sensitive to local terrain effects. This can be seen when comparing with nearby ASOS/AWOS stations in Table 3, and when examining hourly and 5-min effects in Fig. 6. By using a 15-min smoothing window, these variations tend to filter out.

WBGT incorporates all components of heat exposure (temperature, humidity, wind, and solar) and is considered to be one

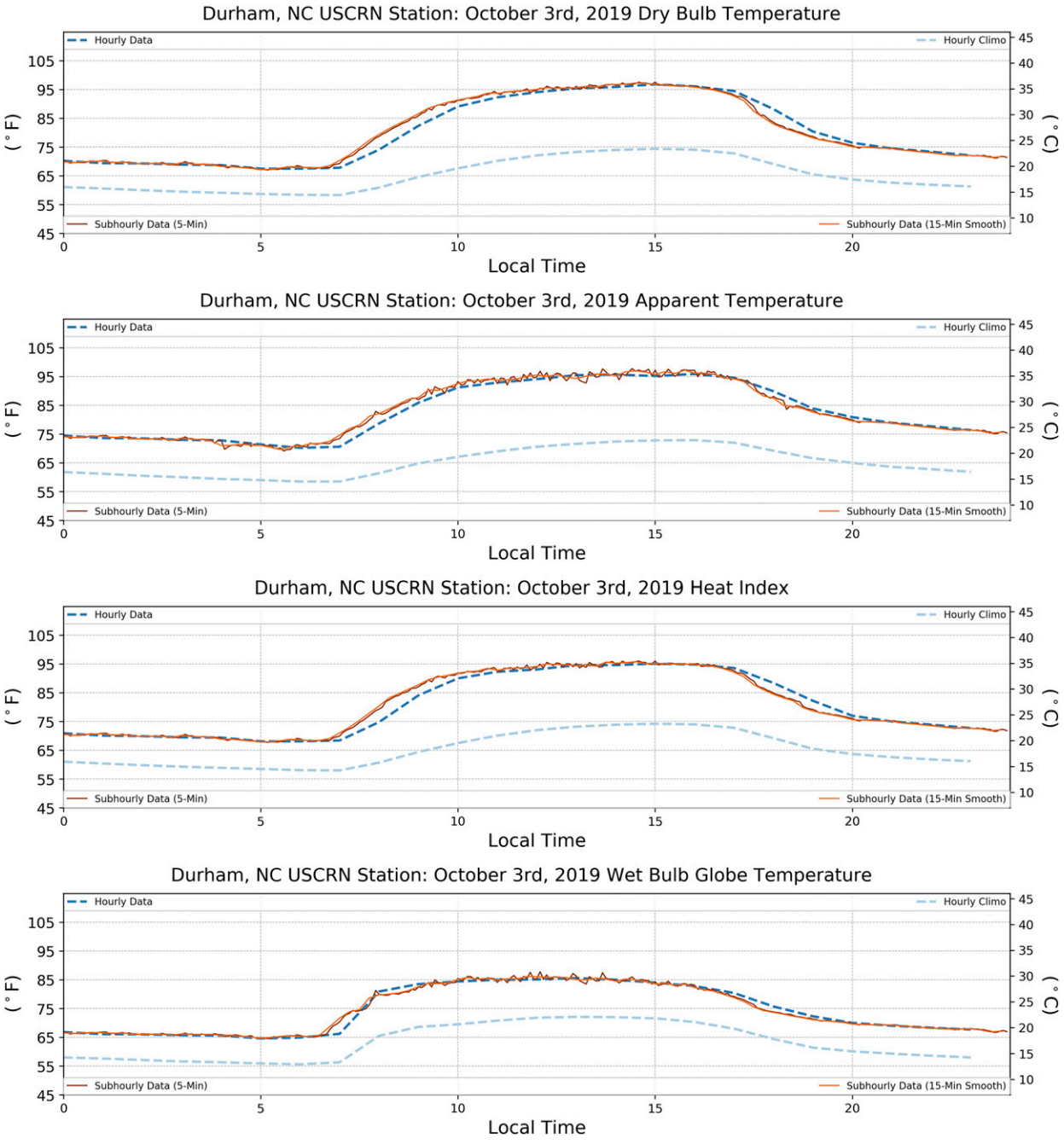

FIG. 6. Time series of T, AT, HI, and WBGT at the Durham USCRN site for 3 Oct 2019. Data include hourly values (dark blue) and climatology (light blue), along with original (brown) and smoothed (orange) 5-min data values.

of the best metrics for outdoor conditions (Lemke and Kjellstrom 2012; Patel et al. 2013). However, it has not been widely used in observational climate studies due to questions about estimation accuracy across diverse climate regions, as well as the lack of black-globe instruments for verification. Direct observations of WBGT and T_g are rare, and while the estimation algorithms of Liljegren et al. (2008) and Dimiceli et al. (2013) prove useful, they were calibrated at selected sites, such as military bases in seven states (Liljegren et al. 2008) and locations around Tulsa (Dimiceli et al. 2013). These methods do not encompass the entire climatological makeup of the United States, and therefore should be recalibrated to reflect varying climates of the United States, especially in the Southeast and Southwest. The Liljegren method was selected for this study because of its successful validation at two sites in North Carolina. While both methods were tested for consistency between USCRN and

TABLE 5. Statistics (°C) on 3 Oct 2019 heat at the Durham USCRN site, including maximum recorded value, standardized (std) anomaly, and percentile thresholds for the month of October.

	Max recorded	Std anomaly	Oct 90th percentile	Oct 95th percentile	Oct 98th percentile
T	36.3	2.5	25.6	27.1	28.5
HI	35.4	2.3	25.7	27.4	29.1
AT	36.4	2.3	25.7	27.3	29.0
WBGT	30.8	1.9	23.7	24.8	25.9

ASOS/AWOS stations nationwide, the North Carolina ECONet was considered to be the more valuable test, because its stations had direct observations of every WBGT variable and were within 5 km of USCRN sites, thus providing the best validation results. Other mesonets outside North Carolina should be incorporated in future validation tests, with appropriate black-globe thermometers and pyranometers installed. Note also that in some cases in which directly observed measures of solar radiation and pressure are not available the reanalysis data are utilized. While the comparisons are deemed acceptable (Table 3), there might be spatial discontinuities, because ERA5 is a 0.25° dataset. This is especially important for solar radiation because there can high variability over short distances, especially in the summer months in the presence of cumulus clouds.

WBGT is highly sensitive to microclimates and can vary by geographic region. Carter et al. (2020) indicated uncertainties in WBGT due to variations in radiation resulting from the degree of site shading, in wind speed resulting from local surface roughness, and in humidity and air temperature because of wetness of the surrounding area. Budd (2008) mentioned issues with WBGT when there is little or no air movement. While WBGT values should be higher with low wind speeds (due to lack of evaporative capacity), this increase is not typically seen. WBGT is also highly sensitive to solar radiation, as can be seen in Fig. 6 and Table 3. Sherwood (2018) noted wind and radiation impacts can vary greatly depending on exactly where someone is located and what clothing they are wearing. Hajizadeh et al. (2017) also noted solar radiation fluctuations, with an R^2 value of 0.233 when comparing sites in Iran. Instantaneous and high temporal resolution values of WBGT can vary greatly. Simplified versions of WBGT (Willett and Sherwood 2012) could be used in these circumstances, which depend on variations in temperature and vapor pressure with assumptions about wind and radiation. Because this simplified version is similar to AT, it is not included here.

b. *Relative versus absolute thresholds*

An important use of these heat metrics is to quantify the severity of threat to human health. Although no single exceedance threshold has proven to be the most effective in determining risk, severity of heat health risk is usually quantified using a variety of absolute (i.e., $\geq n°$) or relative ($\geq n$th percentile) limits. Currently, the NWS applies absolute thresholds in many places across the United States (Hawkins et al. 2017). This threshold is unchanged, regardless of time of year or other characteristics such as local sensitivity and adaptive capacity. Other studies (Meehl and Tebaldi 2004; Grundstein et al. 2015) have shown relative thresholds often provide a better understanding of local heat severity. Additionally, Grundstein et al. (2018) showed relative thresholds are important when considering fatal exertional heat stroke deaths. Using USCRN derived climatologies of HI, AT, and WBGT, an analysis of absolute and relative thresholds is performed. Results show more events are captured when using relative thresholds (Fig. 5, Table 4), especially outside the summer months. The North Carolina heat event in October 2019 had unprecedented HI values at the USCRN site (35.4°C or 95.8°F), which was 6.3°C above the 98th percentile for October (29.1°C or 84.4°F). However, because the HI needs to be at least 40.6°C (105.0°F), no heat-related outlook was provided by the NWS. If a percentile-based method were utilized, information could have been sent to proper organizations, such as athletics and emergency managers, to take appropriate precautions. This issue is not tied to one single event or year. Figure 7 shows the monthly summary of hours above a certain relative or absolute HI threshold in Asheville, a mountainous area that generally experiences cooler temperatures than the lowlands of the state. Heat indices very rarely get to 35.0°C (95.0°F) but often exceed the 90th, 95th, or 98th percentile.

A serious consideration should be made for applying relative thresholds, but that does not mean it will not come with its own complications. Percentile thresholds here are utilized from the stations period of record, which can range between 3 and 11 years. Not only are distributions based on varying years, there also is no consensus on the appropriate number of years needed (i.e., 5 vs 30 years). For a better conceptualization of the station's climate, thresholds should be recalculated with a consistent number of years, and on an annual basis, to reflect the most updated conditions. This will systematically introduce a bias in analyzing events over time, since the thresholds could change each year. Also, fixed numbers are easier to communicate to the public. People comprehend fixed numbers (35.0°C) better than a statistical percentile (98th) and might take more action if they know the number is substantial. Absolute thresholds are still important to incorporate, as well as allowing for warning rules to change with the seasons. For example, one may exceed a 98th-percentile temperature in late autumn and not reach a physiologically severe heat exposure. Likewise, the same level of heat exposure in the late spring as opposed to autumn might have more deleterious impacts on human because they have not yet acclimatized to the onset of summer conditions. Therefore, percentile-based thresholds may need to be graduated with season if used to provide heat exposure warnings to the public.

c. *Communicating WBGT*

WBGT has been widely used in recent years, especially within the NWS. WFOs in Oklahoma, North Carolina, and elsewhere

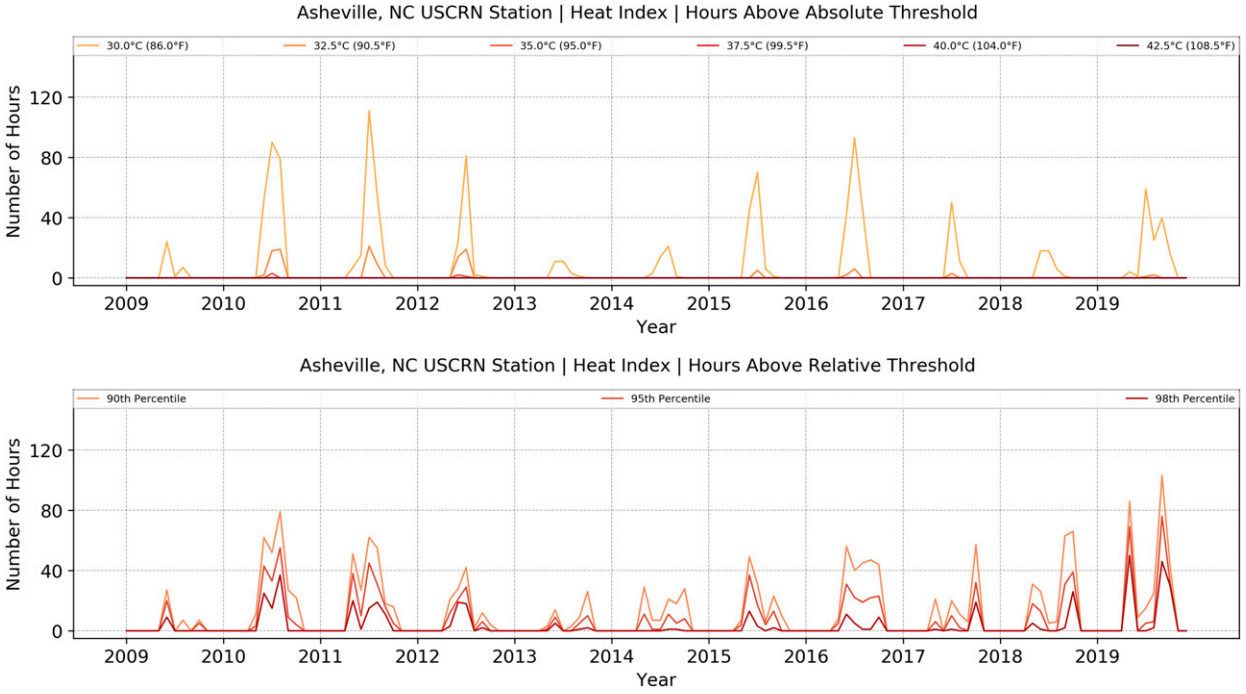

FIG. 7. Number of hours in a given month the HI is above (top) an absolute threshold or (bottom) a relative threshold, from 2009 to 2019 for a USCRN station in Asheville.

are utilizing WBGT in their heat safety messaging. NWS forecast models, such as the National Digital Forecast Database (NDFD) have also begun to compute WBGT nationally. Despite recent successes, communicating WBGT can be a challenge. While WBGT exists on the same scale as other heat metrics (Fahrenheit or Celsius), values tend to be reported in a lower range, creating a problem with human recognition of dangerous WBGT values. Recall that WBGT requires T, T_w, and T_g. The weighting of T_w (70%) is much higher than that of T and T_g (10% and 20%, respectively). Since T_w is the temperature a parcel needs to cool down to for saturation, T_w (and thus, WBGT) are lower than the standard temperature. Table 4 and 5 indicate very dangerous conditions are reached at or above a WBGT of 32.2°C (90.0°F), but the range of WBGT values is considerably lower than HI values for the same temperature and humidity. Figure 8 indicates WBGT values virtually never occur above 32.5°C (90.5°F) in Asheville. This can create public confusion in any location since people might associate these temperatures as a nonthreatening situation. This is consistent with results of Grundstein et al. (2015), who updated a categorical system of WBGT for use originally proposed by the ACSM and GHSA. The WBGT severity categories for the southeastern United States range between 25.7°C (78.2°F) and 32.2°C (90.0°F). According to their work, values above 32.2°C (90.0°F) are indicated as an extreme, life threatening value of WBGT, and all outdoor exercise should be cancelled. However, a similar value of HI is not considered a threat, and the public may attempt to apply this thinking to WBGT.

Adoption of WBGT heat exposure measure in a widespread fashion will be a communication challenge, and the role of social science will be extremely important. One of the ways to overcome this challenge is to provide categorical risk information rather than numerical values, similar to the U.S. Drought Monitor (USDM; Svoboda et al. 2002). Without providing specific numbers, the USDM displays results by categorical risk (e.g., D0, D1) to indicate stages of drought. These categories are based upon underlying drought data and its characteristics, and different precautions are considered for each level. In theory, a similar method could be applied to WBGT or any heat exposure metric, such as H0 or H1. These levels could be based on relative thresholds, which already take into account geography and seasonality. Grundstein et al. 2015 updated categorical risks using percentile thresholds of WBGT to quantify the value in the context of athletic activities. This categorical approach, using relative thresholds, has been widely used by athletic organizations for warm-season sporting operations. Other organizations, such as the Southeast Regional Climate Center (SERCC), the NCSCO, and the NWS Office in Raleigh, North Carolina, have already adopted this categorical method. A similar approach could be utilized using USCRN data, but other sectors should be considered in addition to athletics (such as agriculture, energy, and health).

6. Conclusions

Three heat exposure variables (HI, AT, and WBGT) were calculated for 139 stations of the USCRN for both hourly and 5-min intervals. Similar computations were made with observations from nearby ASOS/AWOS and mesonet stations; when compared, the methodologies produced consistent

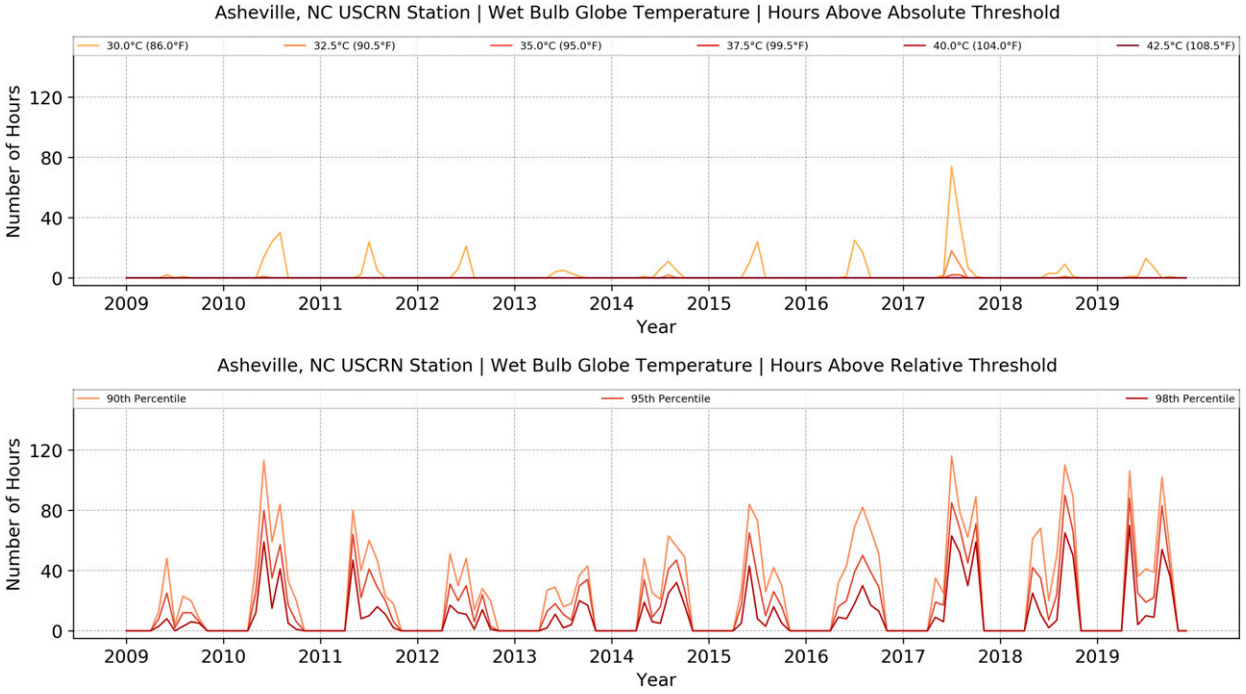

FIG. 8. As in Fig. 7, but for WBGT.

results between networks, with correlation coefficients generally above 0.77. A derived product consisting of these measures of heat exposure in the USCRN beginning in 2009 is available for public access. From these data, hourly climatologies are calculated at each site, using a 15-day window explained by Applequist et al. (2012) to incorporate as many data as possible for stations with short time periods. From these climatologies, the mean, and distribution percentiles (90th, 95th, and 98th) are calculated, and are also publicly available. A case study in the southeastern United States was investigated, and challenges in communicating heat exposure and severity still exist, regardless of which metric used.

While this work mainly focused on USCRN stations, the underlying algorithms can be used at any site that records standard meteorological variables. The paired analysis with ASOS/AWOS stations in the validation portion of the study indicates that these methods could be applied to over 2000 airport stations across the country. While estimations of HI, AT, and WBGT are made at both ASOS and USCRN sites, a comparison of its input variables (Table 3) shows that results are adequate and could be expanded to the entire ASOS network. Moreover, sensitivity in these results could be used to aid calibration of future T_g and WBGT estimations, including those provided by Liljegren et al. (2008) and Dimiceli et al. (2013). In addition, other networks and mesonets, including ones operated by the U.S. Department of Defense, have begun installing black-globe thermometers at some of their sites, so direct measures of WBGT can be made at more locations and estimation methods improved with these more spatially distributed data. A dataset of HI, AT, and WBGT observations can be developed from directly observed conditions measured using standard instrumentation and reanalysis data to fill in data gaps. In addition to point observations, gridded data developed from in situ measurements, including NCEI's nClimGrid (Vose et al. 2014), can be used to calculate a high spatial resolution version of HI, AT, and WBGT. This gridded dataset can be compared to reanalysis datasets, such as ERA5, and even forecast products, including the NWS NDFD, which currently has HI installed, along with WBGT as an experimental product.

Work continues to link these derived heat exposure variables to the vulnerability of people to heat in North Carolina and the southeastern United States. Characteristics of heat vulnerability can be determined through the analysis of multiple census variables indicative of socioeconomic circumstances, living conditions, age and/or disability, and health (Reid et al. 2009). Weighting station or gridded measures of heat exposure by vulnerability can lead to improved understanding of previous heat-wave events that impacted society and help to prepare the adaptive capacity to respond faster and more effectively to future events.

While some communication issues were discussed earlier, more work needs to be done not only to make the heat exposure measurements more understandable, but also to improve the public response to dangerous heat events. Members of the weather and climate enterprise need to work together alongside epidemiologists and emergency managers in order to improve upon the messaging of forecasts and mitigation recommendations. This is especially true if an agency utilizes WBGT, which can typically have lower values compared to related HI and AT. By combining useful thresholds for heat severity, locating populations vulnerable to this exposure, and effectively

communicating the forecast and precautions, it is believed lives will be saved.

Acknowledgments. This work was supported by NOAA through the Cooperative Institute for Satellite Earth System Studies under Cooperative Agreement NA19NES4320002. The authors thank Jay Lawrimore, Scott Stevens, and the anonymous reviewers for their comments.

Data availability statement. The heat exposure product used in this study is derived from the USCRN (Diamond et al. 2013). The hourly and 5-min versions of USCRN were used between 2009 and 2019, and the data are openly available from the NOAA/NCEI (https://www.ncdc.noaa.gov/crn/qcdatasets.html). For the validation study, stations from the ASOS and AWOS networks were taken from the ISD (Smith et al. 2011). Hourly data were used between 2009 and 2019, and the data are openly available from NOAA/NCEI (https://www.ncdc.noaa.gov/isd/data-access). Hourly data were also taken from the ECONet, operated by the NCSCO, and these data are publicly available online (https://climate.ncsu.edu/cronos). Hourly reanalysis data were retrieved from ERA5, provided by the ECMWF (Copernicus Climate Change Service 2017). Although a user account is required, the data are free and available from the Copernicus Climate Data Store (https://cds.climate.copernicus.eu/cdsapp#!/dataset/reanalysis-era5-single-levels).

REFERENCES

Applequist, S., A. Arguez, I. Durre, M. F. Squires, R. S. Vose, and X. Yin, 2012: 1981–2010 US hourly normals. *Bull. Amer. Meteor. Soc.*, **93**, 1637–1640, https://doi.org/10.1175/BAMS-D-11-00173.1.

Arguez, A., I. Durre, S. Applequist, R. S. Vose, M. F. Squires, X. Yin, R. R. Heim Jr., and T. W. Owen, 2012: NOAA's 1981–2010 US Climate normals: An overview. *Bull. Amer. Meteor. Soc.*, **93**, 1687–1697, https://doi.org/10.1175/BAMS-D-11-00197.1.

Budd, G. M., 2008: Wet-bulb globe temperature (WBGT)—Its history and its limitations. *J. Sci. Med. Sport*, **11**, 20–32, https://doi.org/10.1016/j.jsams.2007.07.003.

Carter, A. W., B. F. Zaitchik, J. M. Gohlke, S. Wang, and M. B. Richardson, 2020: Methods for estimating wet bulb globe temperature from remote and low-cost data: A comparative study in central Alabama. *GeoHealth*, **4**, e2019GH000231, https://doi.org/10.1029/2019GH000231.

Copernicus Climate Change Service, 2017: ERA5: Fifth generation of ECMWF atmospheric reanalyses of the global climate. Copernicus Climate Change Service Climate Data Store, accessed 23 May 2020, https://cds.climate.copernicus.eu/cdsapp#!/home.

Curriero, F. S., K. S. Heiner, J. M. Samet, S. L. Zeger, L. Strug, and J. A. Patz, 2002: Temperature and mortality in 11 cities of the eastern United States. *Amer. J. Epidemiol.*, **155**, 80–87, https://doi.org/10.1093/aje/155.1.80.

Diamond, H. J., and Coauthors, 2013: U.S. Climate Reference Network after one decade of operations. *Bull. Amer. Meteor. Soc.*, **94**, 485–498, https://doi.org/10.1175/BAMS-D-12-00170.1.

Dimiceli, V. E., S. F. Piltz, and S. A. Amburn, 2013: Black globe temperature estimate for the WBGT index. *IAENG Transactions on Engineering Technologies*, H. Kim, S. Ao, and B. Rieger, Eds., Springer, 323–334, https://doi.org/10.1007/978-94-007-4786-9_26.

Grundstein, A., and J. Dowd, 2011: Trends in extreme apparent temperatures over the United States, 1949–2010. *J. Appl. Meteor. Climatol.*, **50**, 1650–1653, https://doi.org/10.1175/JAMC-D-11-063.1.

——, C. Williams, M. Phan, and E. Cooper, 2015: Regional heat safety thresholds for athletics in the contiguous United States. *Appl. Geogr.*, **56**, 55–60, https://doi.org/10.1016/j.apgeog.2014.10.014.

——, Y. Hosokawa, and D. J. Casa, 2018: Fatal exertional heat stroke and American football players: The need for regional heat-safety guidelines. *J. Athl. Train.*, **53**, 43–50, https://doi.org/10.4085/1062-6050-445-16.

Habeeb, D., J. Vargo, and B. Stone, 2015: Rising heat wave trends in large US cities. *Nat. Hazards*, **76**, 1651–1665, https://doi.org/10.1007/s11069-014-1563-z.

Hajizadeh, R., S. Farhang Dehghan, F. Golbabaei, S. M. Jafari, and M. Karajizadeh, 2017: Offering a model for estimating black globe temperature according to meteorological measurements. *Meteor. Appl.*, **24**, 303–307, https://doi.org/10.1002/met.1631.

Hawkins, M. D., V. Brown, and J. Ferrell, 2017: Assessment of NOAA National Weather Service methods to warn for extreme heat events. *Wea. Climate Soc.*, **9**, 5–13, https://doi.org/10.1175/WCAS-D-15-0037.1.

Heo, S., M. L. Bell, and J. Lee, 2019: Comparison of health risks by heat wave definition: Applicability of wet-bulb globe temperature for heat wave criteria. *Environ. Res.*, **168**, 158–170, https://doi.org/10.1016/j.envres.2018.09.032.

Holder, C., R. Boyles, A. Syed, D. Niyogi, and S. Raman, 2006: Comparison of collocated automated (NCECONet) and manual (COOP) climate observations in North Carolina. *J. Atmos. Oceanic Technol.*, **23**, 671–682, https://doi.org/10.1175/JTECH1873.1.

Iowa Environmental Mesonet, 2020: UGC or polygon SBW statistics for watch/warning/advisory by state/wfo (#90). Iowa State University Automated Data Plotter, accessed 12 November 2020, http://mesonet.agron.iastate.edu/plotting/auto/?q=90.

Kalkstein, L. S., and R. E. Davis, 1989: Weather and human mortality: An evaluation of demographic and interregional responses in the United States. *Ann. Assoc. Amer. Geogr.*, **79**, 44–64, https://doi.org/10.1111/j.1467-8306.1989.tb00249.x.

Keellings, D. and H. Moradkhani, 2020: Spatiotemporal evolution of heat wave severity and coverage across the United States. *Geophys. Res. Lett.*, **47**, e2020GL087097, https://doi.org/10.1029/2020GL087097.

Leeper, R. D., J. E. Bell, and M. A. Palecki, 2019: A description and evaluation of U.S. Climate Reference Network standardized soil moisture dataset. *J. Appl. Meteor. Climatol.*, **58**, 1417–1428, https://doi.org/10.1175/JAMC-D-18-0269.1.

Lemke, B., and T. Kjellstrom, 2012: Calculating workplace WBGT from meteorological data: A tool for climate change assessment. *Ind. Health*, **50**, 267–278, https://doi.org/10.2486/indhealth.MS1352.

Liljegren, J. C., R. A. Carhart, P. Lawday, S. Tschopp, and R. Sharp, 2008: Modeling the wet bulb globe temperature using standard meteorological measurements. *J. Occup. Environ. Hyg.*, **5**, 645–655, https://doi.org/10.1080/15459620802310770.

Limaye, V. S., J. Vargo, M. Harkey, T. Holloway, and J. A. Patz, 2018: Climate change and heat-related excess mortality in the eastern USA. *EcoHealth*, **15**, 485–496, https://doi.org/10.1007/s10393-018-1363-0.

Maier, G., A. Grundstein, W. Jang, C. Li, L. P. Naeher, and M. Shepherd, 2014: Assessing the performance of a vulnerability index during oppressive heat across Georgia, United States.

Wea. Climate Soc., **6**, 253–263, https://doi.org/10.1175/WCAS-D-13-00037.1.

Meehl, G. A., and C. Tebaldi, 2004: More intense, more frequent, and longer lasting heat waves in the 21st century. *Science*, **305**, 994–997, https://doi.org/10.1126/science.1098704.

Menne, M. J., I. Durre, R. S. Vose, B. E. Gleason, and T. G. Houston, 2012: An overview of the Global Historical Climatology Network-Daily database. *J. Atmos. Oceanic Technol.*, **29**, 897–910, https://doi.org/10.1175/JTECH-D-11-00103.1.

Mora, C., and Coauthors, 2017: Global risk of deadly heat. *Nat. Climate Change*, **7**, 501–506, https://doi.org/10.1038/nclimate3322.

National Academies of Sciences, Engineering, and Medicine, 2017: *Attribution of Extreme Weather Events in the Context of Climate Change*. National Academies Press, 186 pp, https://doi.org/10.17226/21852.

Nicholls, N., C. Skinner, M. Loughnan, and N. Tapper, 2008: A simple heat alert system for Melbourne, Australia. *Int. J. Biometeor.*, **52**, 375–384, https://doi.org/10.1007/s00484-007-0132-5.

Nissan, H., K. Burkart, E. Coughlan de Perez, M. Van Aalst, and S. Mason, 2017: Defining and predicting heat waves in Bangladesh. *J. Appl. Meteor. Climatol.*, **56**, 2653–2670, https://doi.org/10.1175/JAMC-D-17-0035.1.

NWS, 2020a: Weather related fatality and injury statistics. NOAA, accessed 25 September 2020, https://www.weather.gov/hazstat/.

——, 2020b: NWS experimental heat risk. NOAA, accessed 25 September 2020, https://www.wrh.noaa.gov/wrh/heatrisk/pdf/HeatRisk_More_Info_Web.pdf.

OSHA, 2021: Heat hazard recognition. OSHA, accessed 11 February 2021, https://www.osha.gov/heat-exposure/hazards.

Pachauri, R. K., and Coauthors, 2014: *Climate Change 2014: Synthesis Report*. Cambridge University Press, 151 pp., https://www.ipcc.ch/site/assets/uploads/2018/02/SYR_AR5_FINAL_full.pdf.

Patel, T. S., M. S. Stephen, P. Mullen, and W. R. Santee, 2013: Comparison of methods for estimating wet-bulb globe temperature index from standard meteorological measurements. *Mil. Med.*, **178**, 926–933, https://doi.org/10.7205/MILMED-D-13-00117.

Perkins, S. E., and L. V. Alexander, 2013: On the measurement of heat waves. *J. Climate*, **26**, 4500–4517, https://doi.org/10.1175/JCLI-D-12-00383.1.

Raymond, C., D. Singh, and R. M. Horton, 2017: Spatiotemporal patterns and synoptics of extreme wet-bulb temperature in the contiguous United States. *J. Geophys. Res. Atmos.*, **122**, 13 108–13 124, https://doi.org/10.1002/2017JD027140.

——, T. Matthews, and R.M. Horton, 2020: The emergence of heat and humidity too severe for human tolerance. *Sci. Adv.*, **6**, eaaw1838, https://doi.org/10.1126/sciadv.aaw1838.

Reid, C. E., M. S. O'Neill, C. J. Gronlund, S. J. Brines, D. G. Brown, A. V. Diez-Roux, and J. Schwartz, 2009: Mapping community determinants of heat vulnerability. *Environ. Health Perspect.*, **117**, 1730–1736, https://doi.org/10.1289/ehp.0900683.

Rennie, J., J. E. Bell, K. E. Kunkel, S. Herring, H. Cullen, and A. M. Abadi, 2019: Development of a submonthly temperature product to monitor near-real-time climate conditions and assess long-term heat events in the United States. *J. Appl. Meteor. Climatol.*, **58**, 2653–2674, https://doi.org/10.1175/JAMC-D-19-0076.1.

Robinson, P. J., 2001: On the definition of a heat wave. *J. Appl. Meteor.*, **40**, 762–775, https://doi.org/10.1175/1520-0450(2001)040<0762:OTDOAH>2.0.CO;2.

Rothfusz, L. P., 1990: The heat index "equation" (or, more than you ever wanted to know about heat index). NWS Southern Region Headquarters Tech. Attachment SR-90-23, 2 pp., https://wonder.cdc.gov/wonder/help/Climate/ta_htindx.PDF.

Sherwood, S. C., 2018: How important is humidity in heat stress? *J. Geophys. Res. Atmos.*, **123**, 11 808–11 810, https://doi.org/10.1029/2018JD028969.

Smith, A., N. Lott, and R. Vose, 2011: The integrated surface database: Recent developments and partnerships. *Bull. Amer. Meteor. Soc.*, **92**, 704–708, https://doi.org/10.1175/2011BAMS3015.1.

Smith, T. T., B. F. Zaitchik, and J. M. Gohlke, 2013: Heat waves in the United States: Definitions, patterns and trends. *Climatic Change*, **118**, 811–825, https://doi.org/10.1007/s10584-012-0659-2.

Steadman, R. G., 1979: The assessment of sultriness. Part I: A temperature–humidity index based on human physiology and clothing science. *J. Appl. Meteor.*, **18**, 861–873, https://doi.org/10.1175/1520-0450(1979)018<0861:TAOSPI>2.0.CO;2.

——, 1984: A universal scale of apparent temperature. *J. Climate Appl. Meteor.*, **23**, 1674–1687, https://doi.org/10.1175/1520-0450(1984)023<1674:AUSOAT>2.0.CO;2.

Stull, R. S., 2011: Wet-bulb temperature from relative humidity and air temperature. *J. Appl. Meteor. Climatol.*, **50**, 2267–2269, https://doi.org/10.1175/JAMC-D-11-0143.1.

Svoboda, M., and Coauthors, 2002: The Drought Monitor. *Bull. Amer. Meteor. Soc.*, **83**, 1181–1190, https://doi.org/10.1175/1520-0477-83.8.1181.

Vaidyanathan, A., S. R. Kegler, S. S. Saha, and J. A. Mulholland, 2016: A statistical framework to evaluate extreme weather definitions from a health perspective: A demonstration based on extreme heat events. *Bull. Amer. Meteor. Soc.*, **97**, 1817–1830, https://doi.org/10.1175/BAMS-D-15-00181.1.

Vose, R. S., and Coauthors, 2014: Improved historical temperature and precipitation time series for U.S. climate divisions. *J. Appl. Meteor. Climatol.*, **53**, 1232–1251, https://doi.org/10.1175/JAMC-D-13-0248.1.

Weinberger, K. R., D. Harris, K. R. Spangler, A. Zanobetti, and G. A. Wellenius, 2020: Estimating the number of excess deaths attributable to heat in 297 United States counties. *Environ. Epidemiol.*, **4**, e096, https://doi.org/10.1097/EE9.0000000000000096.

Willett, K. M., and S. Sherwood, 2012: Exceedance of heat index thresholds for 15 regions under a warming climate using the wet-bulb globe temperature. *Int. J. Climatol.*, **32**, 161–177, https://doi.org/10.1002/joc.2257.

Wuebbles, D. J., D. W. Fahey, K. A. Hibbard, D. J. Dokken, B. C. Stewart, and T. K. Maycock, Eds., 2017: *Climate Science Special Report: Fourth National Climate Assessment*. Vol. I, U.S. Global Change Research Program, 470 pp., https://doi.org/10.7930/J0J964J6.

Yaglou, C. P., and D. Minard, 1957: Control of heat casualties at military training centers. *Amer. Med. Assoc. Arch. Ind. Health*, **16**, 302–316.